Suppression of Transport of an Interacting Elongated Bose-Einstein Condensate in a Random Potential

D. Clément,[1] A. F. Varón,[1] M. Hugbart,[1] J. A. Retter,[1] P. Bouyer,[1] L. Sanchez-Palencia,[1] D. M. Gangardt,[2]
G. V. Shlyapnikov,[2,3] and A. Aspect[1]

[1]*Laboratoire Charles Fabry, Institut d'Optique, Université Paris-Sud XI, 91403 Orsay Cedex, France*
[2]*Laboratoire de Physique Théorique et Modèles Statistiques, Université Paris-Sud XI, 91405 Orsay Cedex, France*
[3]*Van der Waals-Zeeman Institute, University of Amsterdam, Valckenierstraat 65/67, 1018 XE Amsterdam, The Netherlands*

We observe the suppression of the 1D transport of an interacting elongated Bose-Einstein condensate in a random potential with an amplitude that is small compared to the typical energy per atom, dominated by the interaction energy. Numerical calculations reproduce our observations well. We propose a scenario for disorder-induced trapping of the condensate in agreement with our findings.

PACS numbers: 03.75.Nt, 05.30.Jp

Atomic Bose-Einstein condensates (BECs) in optical potentials are a remarkable system in which to revisit standard problems of condensed matter physics, e.g., superfluidity and quantum vortices, the superfluid to Mott insulator transition, or Josephson arrays [1]. Another important topic in condensed matter physics is that of transport in disordered materials, with relevance to normal metallic conduction, superconductivity and superfluid flow in low temperature quantum liquids. This is a difficult problem and it has led to the introduction of intriguing and nonintuitive concepts, e.g., Anderson localization [2,3], percolation [4], and Bose [5] and spin [6] glasses. It also has a counterpart in wave physics, e.g., in optics and acoustics, specifically coherent diffusion in random media [7]. The main difficulty in understanding quantum transport arises from the subtle interplay of interference, scattering onto the potential landscape, and (whenever present) interparticle interactions.

Transport properties of BECs in periodic optical lattices have been widely investigated, showing lattice-induced reduction of mobility [8–10] and self-trapping [11]. Within the context of random potentials, most of the recent theoretical efforts [12] have considered disordered or quasidisordered optical lattices where a large variety of phenomena have been discussed, such as the Bose-glass phase transition [13], localization [13,14], and the formation of Fermi-glass, quantum percolating, and spin-glass phases in Fermi-Bose mixtures [12,15]. Effects of disorder on BECs have also been addressed in connection with superfluid flows in liquid helium in porous media [16]. In particular, the depletions of the condensate and of the superfluid fractions have been calculated in Ref. [17], and a significant shift and damping of sound waves have been predicted in Ref. [18]. Apart from the (undesired) fragmentation effect of a rough potential on trapped cold atoms and BECs on atom chips [19], there are few experiments on BECs in random potentials [20].

In this Letter we report on the strong reduction of mobility of atoms in an elongated BEC in a random

potential [21]. Starting from a BEC in a 3D highly elongated harmonic trap, we turn off the axial trapping potential while maintaining strong transverse confinement, and we monitor both (i) the axial expansion driven by the repulsive interactions and (ii) the motion of the center of mass of the BEC. When the BEC is subjected to a 1D random potential created by laser speckle, the axial expansion is strongly inhibited and the BEC eventually stops expanding (see Fig. 1). The final rms size L decreases as the standard deviation σ_V of the random potential increases. The same effect has been observed for various realizations of the random potential. We also observe that the center of mass motion provoked by a longitudinal magnetic "kick" at the time of release is strongly damped and is stopped in about the same time (see Fig. 1). These
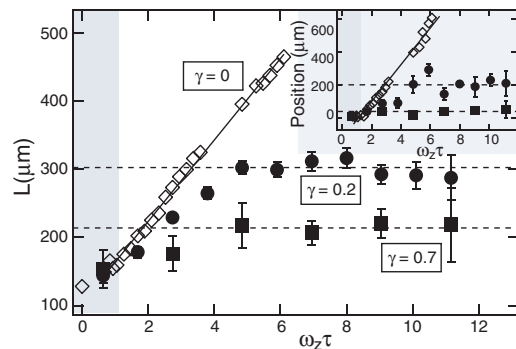

FIG. 1 (color online). Time evolution of the axial rms size L of the BEC, for various amplitudes σ_V of the random potential, all smaller than the chemical potential $\mu[\gamma = \sigma_V/\mu = 0$ ($\diamond$), 0.2 ($\bullet$), and 0.7 ($\blacksquare$)]. The axial trapping frequency is initially $\omega_z/2\pi = 6.7$ Hz and is relaxed during the first 30 ms ($\omega_z\tau < 1.26$) of the expansion time (gray band). Each point corresponds to an average over three measurements; error bars represent 1 standard deviation. The solid lines are linear fits to the data and the dashed lines are guides to the eye. Inset: Motion of the center of mass of the BEC during axial expansion for the same values of γ. Both sets of data show a strong suppression of transport of the BEC in the presence of disorder.

observations are *not* made in a regime of tight binding; i.e., we observe this localization effect [22] for amplitudes of the random potential which are small compared to the chemical potential. One may wonder whether our observations can be interpreted in terms of Anderson localization [2]. In fact, in our situation, the interaction energy plays a crucial role, and the healing length is smaller than the typical distance between the speckle grains. This implies a different scenario, which we discuss in this Letter.

We create an elongated ^{87}Rb BEC in an iron-core electromagnet Ioffe-Pritchard trap [23,24] with oscillation frequencies, $\omega_\perp/2\pi = 660(4)$ Hz radially and $\omega_z/2\pi = 6.70(7)$ Hz axially. BECs of typically 3.5×10^5 atoms are obtained, with Thomas-Fermi (TF) half-length $L_{TF} = 150$ μm and radius $R_{TF} = 1.5$ μm, and chemical potential $\mu/2\pi\hbar \sim 5$ kHz [25]. The random potential is turned on at the end of the evaporative cooling ramp and we further evaporate during 200 ms to ensure that the BEC is in equilibrium in the combined harmonic plus random trap at the end of the sequence. To create the random potential, a $P \leq 150$ mW blue detuned laser beam with optical wavelength $\lambda \simeq 780$ nm, perpendicular to axis z, is shone through a scattering plate and projects a speckle pattern [28] on the BEC (see Fig. 2). The scattered beam diverges to an rms radius of 1.83 mm at the BEC.

A speckle field is defined by (i) a random intensity $I(\mathbf{r})$ with exponential statistical distribution for which the standard deviation equals the average intensity $\sigma_I = \langle I \rangle$ and (ii) an intensity correlation length Δz, defined as the "half-width" of the autocorrelation function [28]:

$$\Delta z = 1.22\lambda l/D, \qquad (1)$$

where D is the beam diameter at the scattering plate and l is the distance from the lens to the BEC. We observe the speckle intensity distribution on a CCD camera placed at the same distance as the atoms. From this, we determine the autocorrelation function to obtain the grain size Δz for various beam diameters D. Taking into account the modulation transfer function [29] of the camera, we find that the measured grain size obeys Eq. (1) to within 2%. For our setup [$l = 140(5)$ mm and $D = 25.4(1)$ mm], Eq. (1) gives $\Delta z = 5.2(2)$ μm. This is much greater than the healing length $\xi = (8\pi na)^{-1/2} = 0.11$ μm of the trapped BEC. Since $R_{TF} < \Delta z \ll L_{TF}$, the optical potential is effectively 1D, with the trapped BEC spread over about 45–50 wells

in the axial direction. We characterize the amplitude of the random potential σ_V with respect to the chemical potential μ by [30]

$$\gamma = \frac{\sigma_V}{\mu} = \frac{2}{3}\frac{\Gamma^2}{2\delta}\frac{\sigma_I}{I_S}\frac{1}{\mu} = \frac{1}{\bar{\omega}}\frac{\Gamma^2}{6\delta}\frac{\sigma_I}{I_S}\left(\frac{15aN}{\overline{a_{ho}}}\right)^{-2/5} \quad (2)$$

with $\bar{\omega} = (\omega_z\omega_\perp^2)^{1/3}$ and $\overline{a_{ho}} = (\hbar/m\bar{\omega})^{1/2}$, m the atomic mass, N the BEC atom number, $I_S = 16.56$ W/m^2 the saturation intensity, $\Gamma/2\pi = 6.01$ MHz the linewidth, $a = 5.31$ nm the scattering length, and δ the laser detuning (between 0.15 nm and 0.39 nm in wavelength). The factor 2/3 accounts for the transition strength for π-polarized light. Taking into account our calibration uncertainty, we measure γ within $\pm 20\%$. For our parameters, the spontaneous scattering time $1/\Gamma_{sc}$ is always larger than 1 s, i.e., much longer than the experiment.

To study the coherent transport of the BEC in the random potential, we open the axial magnetic trap while keeping the transverse confinement and the random potential unchanged. After lowering the current in the axial excitation coils, the axial trapping frequency $\omega_z/2\pi$ is smaller than 1 Hz [31]. Opening the trap abruptly induces atom loss and heating, therefore the trap is opened in 30 ms to avoid these processes. Once the current in the axial coils has reached its final value we have a BEC of $N \sim 2.5 \times 10^5$–3×10^5 atoms in the magnetic guide.

After a total axial expansion time τ (which includes the 30 ms opening time), we turn off all remaining fields (including the random potential) and wait a further 15 ms of free fall before imaging the atoms by absorption. During this time-of-flight, the axial rms size of the BEC does not increase more than 5%. From profiles of the absorption images we evaluate the axial rms size L [32] which we plot in Fig. 1 versus the axial expansion time τ. In the absence of the random potential ($\gamma = 0$), we observe that the rms size L grows linearly at a velocity $v_{rms} \sim 2.47(3)$ mm s^{-1} in agreement with the scaling theory [33]. In the presence of the random potential, the expansion dynamics changes dramatically. For a sufficiently high amplitude, the expansion is significantly reduced and the BEC eventually stops expanding. In addition, we observe the damping of longitudinal motion of the center of mass of the BEC (see inset
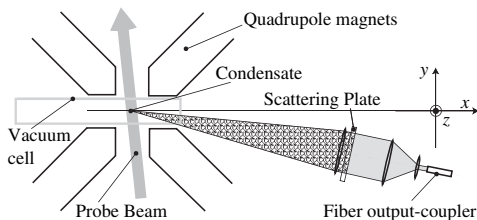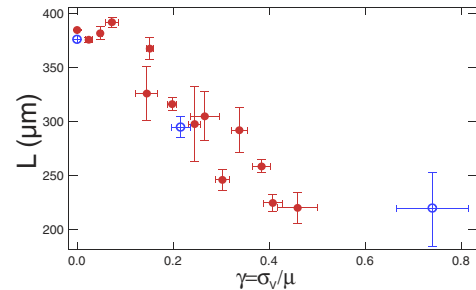

FIG. 2. Optical setup used to create the random speckle potential. The BEC is at the focus of the lens system with its long axis oriented along the z direction.

FIG. 3 (color online). rms size L of the BEC versus γ after an axial expansion time $\omega_z\tau = 4.84$ ($\tau = 115$ ms). The open circles correspond to the curves of Fig. 1.

of Fig. 1). This motion is triggered by an axial magnetic kick during the opening of the trap.

These results show a transition from noninhibited to inhibited transport as the speckle amplitude is increased. This is studied in further detail by measuring the BEC rms size after a fixed axial expansion time of 115 ms ($\omega_z\tau = 4.84$) for different amplitudes σ_V of the random potential. The results are shown in Fig. 3. We see that above a value $\gamma = 0.15$, the rms size decreases with γ.

From the absorption images, we also evaluate the density in the magnetic guide, after correcting for radial expansion during the time of flight. We observe that the density at the center of the BEC does not drop by more than a factor of 2 for $\gamma > 0.2$. Therefore, we conclude that the interaction energy dominates at the center of the BEC trapped by disorder, a point we discuss below.

To understand the disorder-induced suppression of expansion of the BEC, we have performed numerical calculations of the BEC dynamics in the Gross-Pitaevskii approach. We consider a BEC trapped in a cylindrically symmetric 3D-harmonic trap with frequencies $\omega_\perp$ and ω_z in the radial and axial directions, respectively. Assuming tight radial confinement ($\hbar\omega_\perp \gg \hbar\omega_z, \mu, k_BT$), the dynamics is reduced to 1D. In addition, the BEC is subjected to a static random potential $V(z) = \sigma_V v(z)$ where $v(z)$ is a numerically generated speckle pattern [28] with $\langle v\rangle^2 = \langle v^2\rangle/2 = 1$. This slightly differs from the experimental situation where the BEC is very elongated but not strictly 1D. However, in the experiment, the BEC is *guided* in a 1D random potential so that the radial size only slightly changes and, due to the different time scales in the axial ($1/\omega_z$) and radial ($1/\omega_\perp \ll 1/\omega_z$) directions, the radial size adapts adiabatically to the axial size. Thus we expect that the 1D simplified model captures the physics of the
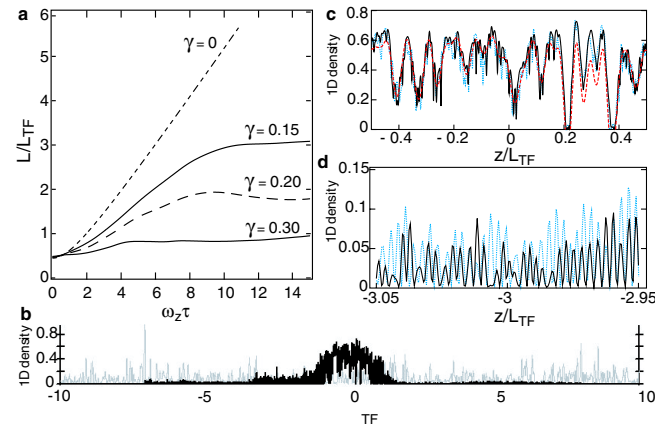

FIG. 4 (color online).   (a) Time evolution of the rms size L of the BEC in the random potential $V(z)$ for various speckle amplitudes $\sigma_V = \gamma\mu$ as obtained from the numerical calculations. (b) Density profile (black) and random potential $V(z)/g_{1D}$ (gray) for $\gamma = 0.2$ at $\omega_z\tau = 10$. (c)–(d) Enlargement of density profile at $\omega_z\tau = 10$ (black solid) and $\omega_z\tau = 20$ [dotted (blue online)]. The dashed (red online) line in (c) is the TF prediction (see text).

experiment. We consider parameters close to the experimental situation (see above). In particular, the healing length ($\xi \simeq 8 \times 10^{-4}L_{TF}$) and the speckle correlation length ($\Delta z \simeq 0.049L_{TF}$) are much smaller than the size of the BEC.

We first compute the static 1D BEC wave function in the combined (harmonic plus random) trap. Because $\xi \ll \Delta z$, the density profile simply follows the modulations of the combined trap in the TF regime: $|\psi(z)|^2 = [\mu - m\omega_z^2z^2/2 - V(z)]/g_{1D}$ in the region where $\mu > m\omega_z^2z^2/2 + V(z)$ and $|\psi(z)|^2 = 0$ elsewhere. Here, m is the atomic mass and $g_{1D} = 2\hbar a\omega_\perp$ the 1D interaction parameter. At time $\tau = 0$, we suddenly switch off the axial harmonic confinement while keeping unchanged the interaction parameter g_{1D} and the random potential, and we compute the time evolution of the BEC. The results for the axial rms size L of the BEC are plotted in Fig. 4(a) for various amplitudes of the random potential. In the absence of disorder, the evolution of the BEC corresponds to self-similar expansion with scaling parameter $b(t) \sim \sqrt{2}\omega_z t$ [34]. In the presence of disorder ($\gamma \gtrsim 0.15$), after initial expansion, the BEC stops expanding. This is qualitatively the same behavior we observed in the experiment. The quantitative agreement is also reasonably good. For example, for $\gamma = 0.2$, the BEC expands by a factor of $\simeq 4$ in the numerics ($\simeq 3$ in the experiment) and is trapped after a transient expansion time of $\omega_z\tau \simeq 8$ ($\omega_z\tau \simeq 6$). This strong suppression of expansion corresponds to disorder-induced trapping of the BEC.

We now describe a scenario for disorder-induced trapping of the BEC. For small amplitudes of disorder, the initial stage of expansion can be described using the scaling theory [33]. According to this, the fast atoms populate the wings of the expanding BEC whereas the slow atoms are close to the center. It is thus tempting to distinguish two regions of the BEC: (i) the center where the interaction energy dominates the kinetic energy and trapping is due to the competition between interactions and disorder, and (ii) the wings where the kinetic energy exceeds the interactions and trapping is rather due to the competition between the kinetic energy and disorder.

In the center, the average density n_0 and thus the effective chemical potential $\bar{\mu}$ slowly decrease during the expansion stage. As the interaction energy is much larger than the kinetic energy, the local density adiabatically follows the instantaneous value of $\bar{\mu}$ in the TF regime: $|\psi(z)|^2 = [\bar{\mu} - V(z)]/g_{1D}$ in the region where $\bar{\mu} > V(z)$ and $|\psi(z)|^2 = 0$ elsewhere. This agrees with our numerical results [see Fig. 4(c)]. This evolution stops with fragmentation, i.e., when the BEC meets two peaks of the random potential with amplitudes larger than $\bar{\mu}$. Using the statistical properties of the random potential [28], we can estimate the probability of such large peaks and we conclude that this happens when n_0 reaches the value

$$n_0 \simeq 1.25\left(\frac{\sigma_V}{g_{1D}}\right)\ln\left[\frac{0.47L_{TF}}{\Delta z}\right]. \qquad (3)$$

Because of the small density, the situation is different in the wings which are populated by almost free particles interacting with the disordered potential. The BEC thus undergoes disorder-induced multiple reflections and transmissions and is ultimately blocked by a large peak of the speckle potential. Therefore, the BEC is not in the TF regime and the local density is not stationary [see Fig. 4(d)]. Because of conservation of energy, the kinetic energy per particle ϵ is of the order of the typical energy in the initial BEC ($\epsilon \sim \mu$) so that the typical wavelength of the fluctuations in the wings is of the order of the healing length in the initial BEC $\lambda_w \sim \xi = \hbar/\sqrt{2m\mu}$.

This scenario is accurately supported by our numerical results [35]. In particular, the density profiles plotted in Fig. 4 show the static TF shape in the center with a density given by Eq. (3) and time-dependent fluctuations in the wings with typical wavelength $\lambda_w \sim \xi$.

In conclusion, we have experimentally investigated transport properties of an interacting BEC in a random potential. Controlling the strength of disorder, we have observed the transition from free expansion to absence of diffusion as disorder increases. We have presented numerical simulations that reproduce well the observed suppression of expansion and we have discussed a theoretical model that describes the scenario for disorder-induced trapping. In the future, it would be interesting to further investigate this highly controllable system, for example, by changing the correlation length of disorder or employing Bragg spectroscopy to probe the momentum spectrum of the BEC [24].

[1] For recent reviews, see J. R. Anglin and W. Ketterle, Nature (London) **416**, 211 (2002).

[2] P. W. Anderson, Phys. Rev. **109**, 1492 (1958).

[3] *Anderson Localization*, edited by Y. Nagaoka and H. Fukuyama, Springer Series in Solid State Sciences Vol. 39 (Springer, Berlin, 1982); *Anderson Localization*, edited by T. Ando and H. Fukuyama, Springer Proc. Phys. Vol. 28 (Springer, Berlin, 1988).

[4] A. Aharony and D. Stauffer, *Introduction to Percolation Theory* (Taylor & Francis, London, 1994).

[5] M. P. A. Fisher *et al.*, Phys. Rev. B **40**, 546 (1989).

[6] M. Mézard, G. Parisi, and M. A. Virasoro, *Spin Glass and Beyond* (World Scientific, Singapore, 1987).

[7] E. Akkermans and G. Montambaux, *Physique Mésoscopique des Électrons et des Photons* (EDP Science ed., Paris, 2004).

[8] S. Burger *et al.*, Phys. Rev. Lett. **86**, 4447 (2001).

[9] M. Krämer *et al.*, Phys. Rev. Lett. **88**, 180404 (2002).

[10] C. D. Fertig *et al.*, Phys. Rev. Lett. **94**, 120403 (2005).

[11] Th. Anker *et al.*, Phys. Rev. Lett. **94**, 020403 (2005); A. Trombettoni and A. Smerzi, *ibid.* **86**, 2353 (2001).

[12] V. Ahufinger *et al.*, cond-mat/0508042.

[13] B. Damski *et al.*, Phys. Rev. Lett. **91**, 080403 (2003).

[14] L. Sanchez-Palencia and L. Santos, cond-mat/0502529 [Phys. Rev. A (to be published)].

[15] A. Sanpera *et al.*, Phys. Rev. Lett. **93**, 040401 (2004).

[16] H. R. Glyde *et al.*, Phys. Rev. Lett. **84**, 2646 (2000).

[17] K. Huang and H. F. Meng, *ibid.* **69**, 644 (1992).

[18] S. Giorgini *et al.*, Phys. Rev. B **49**, 12 938 (1994).

[19] See for example J. Estève *et al.*, Phys. Rev. A **70**, 043629 (2004) and references therein.

[20] J. E. Lye *et al.*, Phys. Rev. Lett. **95**, 070401 (2005).

[21] While writing this paper, we have been informed that similar systems are currently studied in the groups of M. Inguscio at LENS and of W. Ertmer in Hannover (private communications).

[22] We use the word "localization" in its "working definition" of absence of diffusion, see B. van Tiggelen, in *Wave Diffusion in Complex Media*, Proceedings of Les Houches Summer School, edited by J. P. Fouque (Kluwer, Dordrecht, 1999).

[23] V. Boyer *et al.*, Phys. Rev. A **62**, 021601(R) (2000).

[24] S. Richard *et al.*, Phys. Rev. Lett. **91**, 010405 (2003).

[25] In elongated traps, thermal phase fluctuations may be important for large enough temperatures [26]. However, here, we estimate the temperature to be 150 nK [27] and therefore the phase coherence length [24] is $L_\phi \sim L_{TF}$, implying that the BEC is almost fully coherent.

[26] D. S. Petrov, G. V. Shlyapnikov, and J. T. M. Walraven, Phys. Rev. Lett. **87**, 050404 (2001).

[27] F. Gerbier *et al.*, Phys. Rev. A **70**, 013607 (2004).

[28] J. W. Goodman, in *Laser Speckle and Related Phenomena*, edited by J.-C. Dainty (Springer-Verlag, Berlin, 1975).

[29] M. Hugbart *et al.*, Eur. Phys. J. D **35**, 155 (2005).

[30] R. Grimm, M. Weidemüller, and Yu. B. Ovchinnikov, *Advances in Atomic, Molecular and Optical Physics*, edited by B. Bederson and H. Walther (Academic Press, London, 2000), Vol. 42, p. 95.

[31] From the variations of the dipole curvature with the current, we estimate the upper bound of $\omega_z/2\pi$ to be ~ 500 mHz, which is compatible with the linear expansion observed in the absence of disorder (see Fig. 1).

[32] The rms axial size is defined $L = \sqrt{\langle (z - \langle z \rangle)^2 \rangle}$ where $\langle \cdot \rangle$ stands for the density-weighted average.

[33] Yu. Kagan, E. L. Surkov, and G. V. Shlyapnikov, Phys. Rev. A **54**, R1753 (1996); Y. Castin and R. Dum, Phys. Rev. Lett. **77**, 5315 (1996).

[34] Our findings are in excellent agreement with the analytic solution of the scaling equations of [33], $\sqrt{b(t)[b(t) - 1]} + \ln[\sqrt{b(t)} + \sqrt{b(t) - 1}] = \sqrt{2}\omega_z t$.

[35] A detailed analysis of these properties will be described in a future publication.